

Studies of Spectroscopic Ellipsometry in $\text{Cd}_{1-x}\text{Mn}_x\text{Te}/\text{CdTe}$ Superlattices

CHEN Chen-Jia(陈辰嘉)^{1*}, WANG Xue-Zhong(王学忠)¹, Vittorio BELLANI², Angiolino STELLA²

¹*School of Physics, Peking University, Beijing 100871*

²*Consorzio Nazionale Interuniversitario per le Scienze Fisiche della Materia (CNISM) and Dipartimento di Fisica "A. Volta", Università degli Studi di Pavia, 27100 Pavia, Italy*

(Received 30 August 2005)

$\text{Cd}_{1-x}\text{Mn}_x\text{Te}/\text{CdTe}$ superlattices and thin films were grown by molecular beam epitaxy on GaAs (001) substrates. Spectroscopic ellipsometry measurements were performed on $\text{Cd}_{1-x}\text{Mn}_x\text{Te}/\text{CdTe}$ superlattices with compositions $x = 0.4, 0.8$, and $\text{Cd}_{1-x}\text{Mn}_x\text{Te}$ thin films with $x = 0.2, 0.4, 0.6$ at room temperature in the photon energy range 1.4–5 eV. In superlattices the pseudodielectric functions measured by ellipsometry show specific features related to the exciton transition between quantized interbands. The exciton transitions related to the heavy holes of 11H, 22H, and 33H are observed and identified. In thin films spectroscopic ellipsometry allows the clear identification of the energy gap E_0 . Additionally, critical point transitions are observable in both the spectra of the superlattices and films. Photorefectance spectra were also performed at room temperature in order to compare with our ellipsometry results. After taking into account the strain-induced and quantum confinement effects, the theoretical calculations are in good agreement with our experimental spectra. Ellipsometry appears to be a suited technique to monitor the MBE growth, ultimately also in situ, of diluted magnetic low-dimensional systems.

PACS: 78.67.Pt, 78.66.Hf, 78.20.Ci

The strong exchange interactions (*sp-d* exchange) and the interactions between localized magnetic ions (*d-d* exchange) in diluted magnetic semiconductor (DMS) $\text{Cd}_{1-x}\text{Mn}_x\text{Te}$ materials lead a series of interesting magnetic-optical properties.^[1,2] The recent development of molecular beam epitaxy (MBE) has allowed us precisely controlled growth of high-quality II–VI diluted magnetic semiconductors (DMS) quantum wells and superlattices (SLs), in which it is possible to control an interacting region between the carrier spin and the magnetic ion spin embedded in the structures, and various spin-dependent optical properties, which open new possibilities for spintronic devices.^[3,4] Spectroscopic ellipsometry (EL) has been recently applied to the study of DMS $\text{Cd}_{1-x}\text{Mn}_x\text{Te}$ thin films.^[5–7] To our knowledge, up to now no study has been published about the ellipsometry response of $\text{Cd}_{1-x}\text{Mn}_x\text{Te}/\text{CdTe}$ SLs.

EL is a spectroscopic optical technique that allows the measurement of the dielectric function of semiconductors from the change of the polarization state of the light after its reflection by the surface of the material under investigation. This technique is frequently used for the in situ real-time monitoring of the MBE growth of semiconductor thin films, heterostructures and low-dimensional systems.^[8] More precisely EL measures the complex reflectance ratio between the polarization states of the reflected and the incident waves, χ_r and χ_i respectively. In the case of an ambient-bulk material interfaces (the two-phase model), this ratio is directly related to the dielectric function of

the material. In SLs, being multi-layered structures, the two-phase model no longer applies. Nevertheless, it is useful and very common to represent the complex reflectance ratio as a pseudodielectric function in the two-phase model. This procedure has been successfully used by to study dielectric and optical properties of GaAs/AlAs SLs.^[9–13]

In this Letter, we present EL results on $\text{Cd}_{1-x}\text{Mn}_x\text{Te}/\text{CdTe}$ SLs with high values of composition range ($x = 0.4, 0.8$), which are related to the interband exciton and critical point (CP) transitions. The effects of a lattice mismatch up to 1.8% between CdTe well and $\text{Cd}_{1-x}\text{Mn}_x\text{Te}$ ($x = 0.8$) barriers are studied by EL. We present EL spectra on $\text{Cd}_{1-x}\text{Mn}_x\text{Te}$ thin films for reference.

$\text{Cd}_{1-x}\text{Mn}_x\text{Te}/\text{CdTe}$ SLs and $\text{Cd}_{1-x}\text{Mn}_x\text{Te}$ films were grown by MBE on GaAs (001) substrates. Two SL samples *A* and *B* comprise 20 periods $\text{Cd}_{1-x}\text{Mn}_x\text{Te}$ ($x = 0.4, 0.8$) barriers of thickness L_b and between CdTe wells of thickness L_w were grown on a 500-nm-thick CdTe buffer layer. The parameters for sample *A* are $x = 0.4$, $L_w = L_b = 14$ nm, and for sample *B* are $x = 0.8$, $L_w = L_b = 10$ nm. The $\text{Cd}_{1-x}\text{Mn}_x\text{Te}$ thin films have a 700-nm thickness and with compositions $x = 0.2, 0.4, 0.6$, respectively.

EL spectra were recorded with an automatic rotating-polarizer spectroscopic ellipsometer (SOPRA MOSS-ES4G) in the spectral range between 1.4 and 5.0 eV with an incidence angle of 75°. The photorelectance (PR) spectrum in thin films with $x = 0.2$ was measured at room temperature using a halogen-lamp

* Email: chenchenjia@yahoo.com or jiachen@pku.edu.cn
©2005 Chinese Physical Society and IOP Publishing Ltd

source. Light was passed through a double monochromator as the probe beam focused onto the sample (placed in a cryostat) by means of a lens. A He-Ne laser line (~ 1 mW, $\lambda_{ex} = 632.8$ nm) was chopped at about 150 Hz as a modulation beam. The reflected beam was collected by a second lens and focused onto the detector. The light striking the detector contains two signals: the dc signal $I_0(\lambda)R(\lambda)$ was measured using a multimeter where $R(\lambda)$ is the dc reflectance of the material. The ac signal from the detector, $I_0(\lambda)\Delta R(\lambda)$ was measured using a lock-in amplifier, where $\Delta R(\lambda)$ is the modulated reflectance. Then the quantity $\Delta R(\lambda)/R(\lambda)$ was recorded by a computer. The complete study of the PR and the photoluminescence (PL) optical emission as a function of temperature in these SLs has been reported in our previous works.^[14,15]

In Fig.1(a) we report a typical result of $\text{Cd}_{1-x}\text{Mn}_x\text{Te}$ thin film sample with $x = 0.2$. pseudodielectric function from 1.4 eV, an energy much lower than the energy gap E_0 of the thin film, up to 5.0 eV, a high enough energy to observe the CP transitions E_1 and $E_1 + \Delta_1$. These CP transitions are labeled accordingly to the Cardona and Greenway notations.^[16] Their energy and shape agree with those of previously reported works.^[5-7]

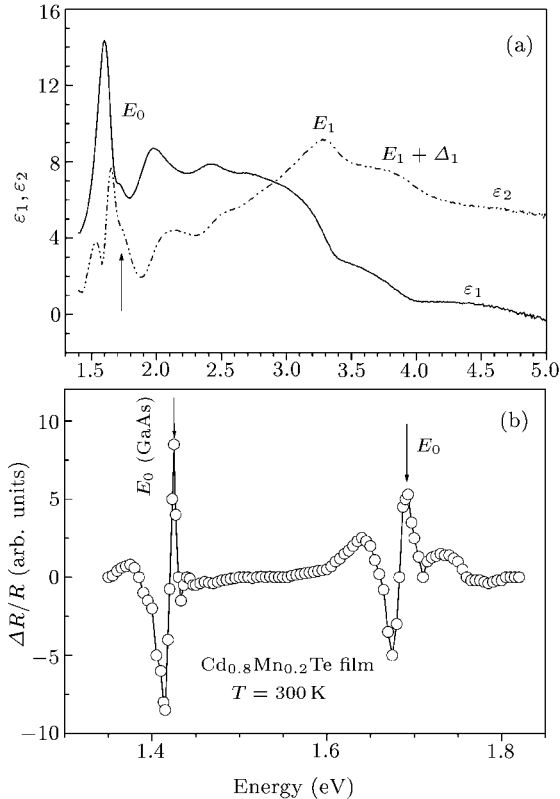


Fig. 1. (a) EL pseudodielectric functions ε_1 and ε_2 of $\text{Cd}_{0.8}\text{Mn}_{0.2}\text{Te}$ thin films; and (b) PR spectrum at room temperature.

In all the three thin-film spectra at low energies,

i.e. below E_0 , we can see a series of oscillations that correspond to interference due to multiple reflections within the film which is transparent at energy below the gap. As the absorption in the film increases, the amplitude of the oscillations decreases. Thus a jump in the amplitude of the oscillations, or their phase, is directly related to a jump in the absorption of the film, that is, to a strong absorption edge.^[9] In fact, at the energy gap E_0 corresponding to the direct transition from the highest valence band to the lowest conduction band at the Γ point ($\Gamma_8 \rightarrow \Gamma_6$), the $\text{Cd}_{1-x}\text{Mn}_x\text{Te}$ film begins adsorbing efficiently the light and preventing it to reach the film/substrate interface, therefore preventing the interference effect. We can clearly see the PR peak in Fig. 1(b) of E_0 (1.686 eV) at the same energy of a small shoulder present both in the pseudodielectric functions ε_1 and ε_2 (Fig. 1(b)).

In all the EL spectra we can also clearly see the CP transitions labeled E_1 and $E_1 + \Delta_1$. Here E_1 corresponds to the transition along the A ($A_{4,5} \rightarrow A_6$) direction, and $E_1 + \Delta_1$ to the spin-orbit (SO) splitting. We can observe that both the transitions progressively smear with the increasing Mn composition. We presume that this behaviour is related to the increase of the disorder with the increase of the random substitution on Cd with the magnetic ion Mn.

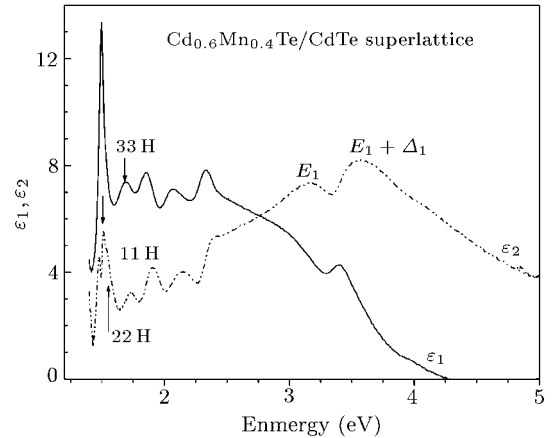


Fig. 2. EL pseudodielectric functions ε_1 and ε_2 of $\text{Cd}_{0.6}\text{Mn}_{0.4}\text{Te}/\text{CdTe}$ SL sample A at room temperature. The arrows identify the theoretical results of exciton transitions.

In Figs.2 and 3 we report the pseudodielectric functions ε_1 and ε_2 obtained on SL samples A and B respectively, and the arrows identify the theoretical results of exciton transitions. We can see a series of oscillations in Figs. 2 and 3, which correspond to interferences due to multiple reflections within the superlattice. When the absorption increases, the amplitude of the oscillations decreases. All the exciton transitions are overlapped on the oscillations region. The EL spectra of the SLs show the features related to the exciton transitions between the quantized va-

lence and conduction interbands, 11 H, 22 H, and 33 H, which correspond to the exciton transitions from the first (ground), second and third conduction subband to the first (ground), second and third heavy subband state, respectively.

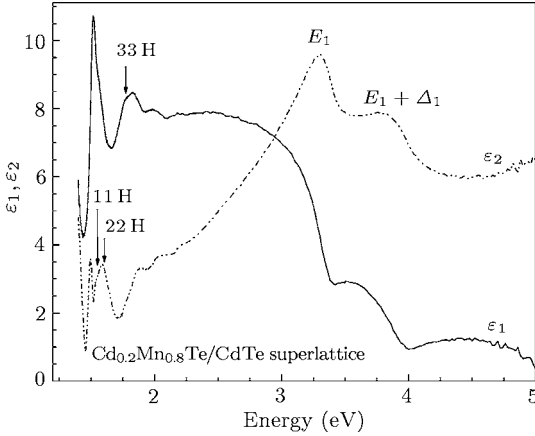


Fig. 3. EL pseudodielectric functions ε_1 and ε_2 of $\text{Cd}_{0.2}\text{Mn}_{0.8}\text{Te}/\text{CdTe}$ SL sample B at room temperature. The arrows identify the theoretical results of exciton transitions.

In order to identify these exciton transitions, we calculate the theoretical values of the interband exciton transitions in the framework of the envelope function approximation,^[14] taking into account the strain effect due to the lattice mismatch between the wells and barriers with different compositions. In regard of the strain, the difference in the lattice parameter gives rise to strains in the SL structure, which strongly modifies the potential profile along the growth direction z . The strain effect, which includes a hydrostatic (a_c, a_v) and a shear component of the stress (b_v), produces shifts in the conduction and valence-band extreme and splits the degeneracy of the heavy and light-hole valence band edge, respectively. For strain along the (001) SLs, the shifts of conduction, heavy and light-hole valence band extremes can be given by $\Delta E_c = -C\varepsilon_{//}a_c$, $\Delta E_{hh} = -C\varepsilon_{//}a_v + C'\varepsilon_{//}b_v$, $\Delta E_{lh} = -C\varepsilon_{//}a_v - C'\varepsilon_{//}b_v$, respectively. In these expressions $C = 2(1 - C_{12}/C_{11})$, $C' = 2(1 + C_{12})/C_{11}$, C_{11} and C_{12} are elastic constants and $a_c = -3.96$ eV, $a_v = 0.55$ eV and $b_v = -1.1$ eV are the deformation potential for CdTe and $\varepsilon_{//}$ is component of the strain tensor parallel to the plane of the interface. After taking into consideration the strain-induced and quantum-confinement effects, the best agreement between theoretical calculation and experimental PR spectra have been obtained using a conduction band offset equal to 0.9 and exciton binding energies of 16 meV and 10 meV for the heavy and light-hole excitons, respectively.

In the EL spectra of SL sample A (see in Fig. 4(a)) we can observe and identify small shoulders both in

ε_1 and ε_2 corresponding to the 11 H and 22 H interband exciton transition and, less resolved, those corresponding to the 33 H interband. These interband exciton transitions have been observed and assigned in the PR spectra,^[14] as shown in Fig. 4(b), at the same energy positions.

We can compare, for instance, the theoretically calculated interband exciton transition energies for sample A at 300 K with the experimental spectra results. Theoretical calculation results give the following values for the exciton transitions: 1.517 eV (11 H), 1.567 eV (22 H), and 1.649 eV (33 H), and we can see in Figs. 4(a) and 4(b) that there is a good agreement between these theoretical values and the experiment energy positions of the transitions with 1.514 eV (11 H), 1.566 eV (22 H), and 1.646 eV (33 H).

At higher energies the EL spectra of these SL samples show the transitions due to the CP transitions E_1 and $E_1 + \Delta_1$ at energies close to those observed in the $\text{Cd}_{1-x}\text{Mn}_x\text{Te}$ thin film samples and with a similar line-shape.

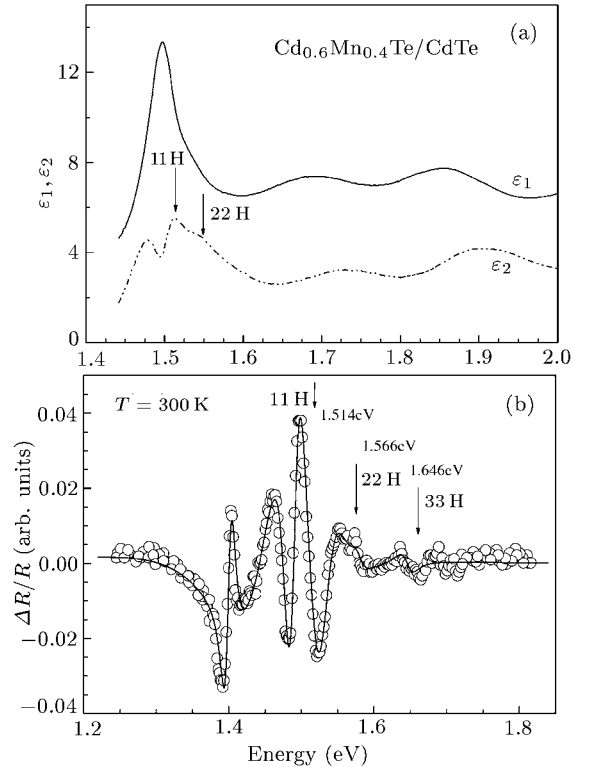


Fig. 4. (a) EL pseudodielectric functions ε_1 and ε_2 of $\text{Cd}_{0.6}\text{Mn}_{0.4}\text{Te}/\text{CdTe}$ SL sample A at room temperature, and (b) PR spectrum (circles) of $\text{Cd}_{0.6}\text{Mn}_{0.4}\text{Te}/\text{CdTe}$ SL sample A at room temperature. The solid line is a line-shape best fit. The arrows identify the exciton transitions.

In Fig. 5(a) we report the EL spectra for SL sample B which has the higher composition of Mn in the barriers ($x = 0.8$). In the EL spectra ε_1 and ε_2 of this sample we can observe and identify up to three interband exciton transitions: 11 H, 22 H and 33 H,

which are related to the shoulders. In Fig. 5(b) we report the PR spectrum for SL sample *B*. The arrows identify the exciton transitions of 11 H, 22 H, and 33 H, which are the same energy position with the EL spectra. Both the spectra of EL and PR are in quite good agreement with the theoretical calculation results: 11 H=1.545 eV, 22 H=1.613 eV and 33 H=1.725 eV.^[14] EL appears thus capable to oversee both the interband exciton and the CP transitions in DMS SLs also for high composition of magnetic ions in one of the constituting semiconductors.

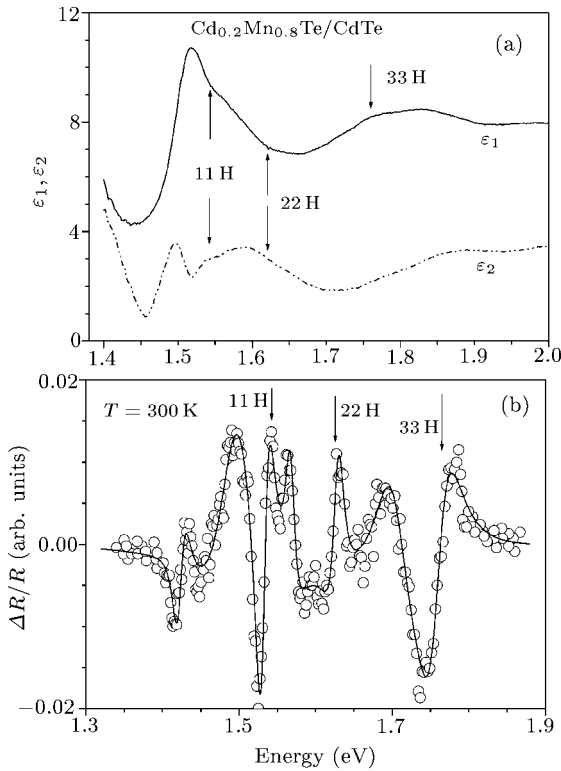


Fig. 5. (a) EL pseudodielectric functions ϵ_1 and ϵ_2 of $\text{Cd}_{0.2}\text{Mn}_{0.8}\text{Te}/\text{CdTe}$ SL sample *B* at room temperature, and (b) PR spectrum (circles) of sample *B* at room temperature. The solid line is a line-shape best fit. The arrows identify the exciton transitions.

In summary, spectroscopic ellipsometry measurements have been performed on $\text{Cd}_{1-x}\text{Mn}_x\text{Te}/\text{CdTe}$ superlattices with compositions $x = 0.4, 0.8$, and $\text{Cd}_{1-x}\text{Mn}_x\text{Te}$ thin films with $x = 0.2, 0.4, 0.6$ at room temperature in the photon energy range 1.4–5 eV. In superlattices the pseudodielectric functions measured

by ellipsometry show specific features related to the exciton transition between quantized interbands. The exciton transitions related to the heavy holes of 11 H, 22 H, and 33 H are observed and identified. In thin films, spectroscopic ellipsometry allows the clear identification of the energy gap E_0 . Additionally, critical point transitions are observable in both the superlattices and films spectra. Compared to photoreflectance spectra and theoretical calculation results, the 11 H, 22 H and 33 H exciton transitions in both the EL and PR spectra are the same energy positions and are in good agreement with the theoretical results. Ellipsometry appears to be a suited technique to monitor the MBE growth, ultimately also in situ, of diluted magnetic low-dimensional systems.

References

- [1] Furdyna J K 1988 *J. Appl. Phys.* **64** R29
- [2] Cheng H H, Nicholas R J, Ashenford D E and Lunn B 1997 *Phys. Rev. B* **56** 10453
- [3] Ohno Y, Young D. K, Beschoten B, Matsukura F, Ohno H and Awschalom D D 1999 *Nature* **402** 792
- [4] Wolf S A, Awschalom D D, Buhrman R A, Daughton J M, von Molnar S, Roukes M L, Chtchelkanova A Y and Treger D M 2001 *Science* **294** 1488
- [5] Wronkowska A A, Wronkowski A, Bukaluk A, Stefanski M, Arwin H, Firszt F, Legowski S, Meczynska H and Hradil K 2003 *Appl. Surf. Sci.* **212** 110
- [6] Hwang Y, Kim H, Chung M, Um Y, Park H and Yoo P 2001 *Jpn. J. Appl. Phys.* **40** 5247
- [7] Chandra S, Malhotra L K and Rastogi A C 2001 *J. Appl. Phys.* **78** 5645
- [8] Azzam R M A and Bashara N M 2003 *Ellipsometry and Polarized Light* (Amsterdam: Elsevier)
- Harland Tompkins G, William A et al 1999 *Spectroscopic Ellipsometry and Reflectometry: A User's Guide* (New York: Wiley)
- [9] Garriga M, Cardona M, Christensen N E, Lautenschlager P, Isu T and Ploog K 1987 *Phys. Rev. B* **36** 3254
- [10] Alouani M, Gopalan S, Garriga M and Christensen N E 1988 *Phys. Rev. Lett.* **61** 1643
- [11] Mo D and Tan J H 1998 *Thin Solid Films* **313-314** 587
- [12] Schmid U, Christensen N E, Cardona M, Lukes F and Ploog K 1992 *Phys. Rev. B* **45** 3546
- [13] Bellani V, Parravicini G B, Diez E, Domínguez-Adame F and Hey R 2002 *Phys. Rev. B* **66** 193310
- [14] Chen C J, Wang X Z, Liang X G, Tavazzi S, Borghesi A, Sassella A, Bellani V, Geddo M and Stella A 2002 *J. Appl. Phys.* **92** 5169
- [15] Bellani V, Stella A, Chen C J, Wang X Z and Liang X G 2005 *J. Appl. Phys.* **97** 083526
- [16] Cardona M and Greenway D L 1963 *Phys. Rev.* **131** 98